Fibers and Polymers 2018, Vol.19, No.4, 751-759
DOI 10.1007/s12221-018-7988-3

ISSN 1229-9197 (print version)
ISSN 1875-0052 (electronic version)

Stretching Deformation Mechanism of Polyacrylonitrile-based Carbon Fiber Structure at High Temperatures

Yu Wang, Tao Yan, Shuai Wu, Yuan-jian Tong, Ai-jun Gao*, and Liang-hua Xu*

National Carbon Fiber Engineering Technology Research Center, Beijing University of Chemical Technology, Beijing 100029, China

(Received November 15, 2017; Revised January 21, 2018; Accepted February 15, 2018)

Abstract: In a high-temperature environment, polyacrylonitrile-based carbon fiber (PAN-CF) can be deformed by stretching, where the stretching deformation ability of PAN-CF is enhanced with the increase of the temperature. Further, the high-temperature stretching deformation of PAN-CF directly affects the control of the carbon crystalline orientation. Based on the techniques of high-resolution transmission electron microscopy (HRTEM), Raman spectroscopy, X-ray diffraction and in situ tension testing, the variation regularity and the intrinsic mechanism of high-temperature stretching deformation ability of PAN-CF obtained at different preparation temperatures were systematically studied in a high-temperature environment. The results indicated that the essence of PAN-CF high-temperature deformation was the relative motion of the carbon crystallite. Further, the main structural parameters that affected the high-temperature stretching deformation ability of PAN-CF were the degree of cross-linking between the carbon crystallites, the orientation angle(OA) of the carbon crystallite and the nitrogen content. When the testing temperature was lower than the preparation temperature, only physical structure changes were observed in the PAN-CF. For the PAN-CF tested undergoing physical structure changes, as the degree of cross-linking between the crystallites and the orientation angle decreased, the slipping of crystallites became easier. In the same environment, as the stretching tension decreased, the stretching deformation ability improved. When PAN-CF was tested under temperatures higher than the preparation temperature, the microcrystalline cross-linking in the PAN-CF was prone to fracture and slipping, and the high-temperature stretching deformation ability was enhanced. Also, for PAN-CF of lower preparation temperatures in PAN-CF containing no nitrogen (i.e., <0.15 wt%), the cross-linkages increased and the structures were more unstable, inducing an increase in the fracture of weak bonds and a reduction of the stretching tension. For nitrogen-containing PAN-CF, the removal of nitrogen led to severe shrinkage in the graphite layer and interlayer, and the fiber tension was thus increased, causing the high-temperature stretching deformation ability of the PAN-CF with less nitrogen content to be improved.

Keywords: Polyacrylonitrile-based carbon fiber, Stretching deformation, Cross-linking structure, Nitrogen element, Orientation angle

Introduction

In the preparation process of polyacrylonitrile-based carbon fibers (PAN-CFs), the carbon crystalline size can be increased by increasing the treatment temperature to realize the high-tensile modulus of PAN-CF but to cause the decrease of its tensile strength [1-5]. It has been found that the carbon crystalline preferential orientation degree can be enhanced by moderate stretching, which can simultaneously achieve an increase of the tensile strength and tensile modulus [6-8] and achieve the preparation of high-strength high-modulus PAN-CF. Therefore, PAN-CF treatment technology is pursuing a small orientation angle of the carbon crystallite. Stretching is an effective method to decrease the carbon crystalline orientation angle of the carbon fiber, but the high-temperature stretching deformation ability of PAN-CF is directly related to its structure.

A characteristic of PAN-CF is its high modulus, and it is nearly undeformable at room temperature. Nevertheless, PAN-CF exhibits relaxation and a certain degree of stretching deformation during high-temperature treatments [9,10]. Previous studies [11,12] have speculated that the high-temperature relaxation of PAN-CF is caused by the high-temperature creep of chaotic graphite structure in the material. The axial tension that arises in the fiber stretching reflects the stretching deformation of the fiber, where lower tension signifies greater deformation ability. However, research on the stretching deformation mechanism of PAN-CF at high temperatures is scarce. In this paper, during the process of physical structure changes in PAN-CF, the relationship between stretching deformation and graphite-like structure at different treatment conditions was systematically studied. Based on the influence that the physical structure change in PAN-CF has on its stretching deformation, the influence of the high-temperature physical and chemical structure changes in PAN-CF on its stretching deformation was also studied.

Experimental

The PAN precursors with 12k (12000 filaments per tow) and a single fiber diameter of about 9.0 μm were provided by the Research Institute of Jilin Petrochina Company, which were made of PAN copolymer with 97.5 wt% acrylonitrile (AN) and 2.5 wt% itaconic acid (IA). The PAN precursor fibers were stabilized and carbonized by a self-

*Corresponding author: bhgaoaijun@163.com
*Corresponding author: xulh@mail.buct.edu.cn

designed pilot production line comprising four stabilization furnaces and two carbonization furnaces. The stabilization furnaces were set as step-wise temperatures of 200-235-255-270 °C and corresponding stretching ratios of 2-1-0-0 %. The PAN fibers were stabilized by passing through all the furnaces for approximately 1 h in air environment with a constant flow rate of 65 *l* min^{-1} for each furnace. The continuous carbonization process consisted of pre-carbonization and carbonization, and the two carbonization process were performed under a nitrogen atmosphere (>99.999 %). During pre-carbonization, the fibers were stretched at a ratio of 3 % in the furnace at 650 °C with the duration of 5 min. During carbonization, the fibers were allowed to shrink to 3 % in the furnace at 1350 °C with the duration of 3 min. The nitrogen gas flow rate was kept at 10 and 5 *l* min^{-1} for the pre-carbonization and carbonization furnaces, respectively. Finally, the carbon fibers were graphitized at 1400-2400 °C under a nitrogen atmosphere (>99.999 %) for 144 s, and the length of the fibers in the graphite furnace was kept constant. The nitrogen gas flow rate was kept at 15 *l* min^{-1} for the graphite furnaces. The PAN-CFs were then wound up using an automatic winder (EKTW-C, KAMITSU, Japan) for testing. The sample labels and their element contents are shown in Table 1.

The high-temperature stretching deformation of the PAN-CF samples listed in Table 1 was studied using the device schematically shown in Figure 1. Using the device, the sample fibers were continuously fed into the furnace by an initial set of rollers (rollers 1) and were collected by a final set of rollers (rollers 2), where the speed of rollers1 and rollers 2 was adjusted to give 144 s of residence time in the graphite furnace. The stretching of the PAN-CFs at high temperature was accomplished by setting different velocities for rollers 1 and rollers 2. The testing conditions of the samples listed in Table 1 are shown in Table 2 and Table 3. The tension of the PAN-CFs in the high-temperature circumstances was measured using a tension meter (DN1-5000, SCHMIDT, Germany), each sample was measured five times, and the mean values were used.

The element content of the PAN-CF samples prepared with different temperatures was obtained using elemental analysis (Vario MICRO CUBE, Elementar Analysensysteme GmbH, Germany). Each sample was measured two times, and the mean values were used.

The chemical structure of the carbon fibers was measured by a Raman spectrometer (RM2000, RENISHAW Plc, UK) attached with an Olympus optical microscope. The excitation light of the Raman spectrometer was provided by a 532-nm laser (Ar ion), and the laser spot size was 0.7 um in diameter. The fibers were fixed on a glass slide. The 50×objective lens of the microscope was used both to focus the laser beam on the specimen and to collect the scattered radiation. The Raman wavelength shifts ranged from 1000 to 1850 cm^{-1}. The fibers were exposed under the laser for 15 s each time, with 10 cumulative exposure times. The Raman spectra were curve-fitted to a Lorentz-Gauss area function using the software of Peak Fit v4.12 to acquire the parameters of peak position, peak area, and full width at half maximum height (FWHM). Each sample was measured five times, and the

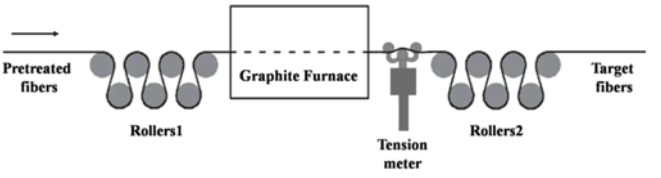

Figure 1. Schematic diagram of the testing apparatus for PAN-CF high-temperature stretching deformation.

Table 1. The PAN-CF sample labels (sample no.) and their element content

Preparation temperature (°C)	2400	2300	2200	2100	1900	1700	1600	1500	1400
Nitrogen content (%)	0.01	0.01	0.03	0.04	0.13	0.82	1.49	1.99	2.48
Hydrogen content (%)	-	-	-	-	0.02	0.04	0.05	0.07	0.11
Carbon content (%)	99.99	99.99	99.97	99.96	99.86	99.14	98.47	97.93	97.42
Sample no.	P-24	P-23	P-22	P-21	P-19	N-17	N-16	N-15	N-14

Table 2. Testing conditions of the PAN-CF with physical structure changes

Sample no.	P-24	P-23	P-22
Testing temperature (°C)	2000/2100/2200/2300/2400	2000/2100/2200/2300	2000/2100/2200
Relative draft ratio (%)	0.0/0.5/1.0/1.5/2.0		

Table 3. Testing conditions of the PAN-CF with physical and chemical structure changes

Sample no.	P-23	P-22	P-21	P-19	N-17	N-16	N-15	N-14
Testing temperature (°C)	2400							
Relative draft ratio (%)	0.0/0.5/1.0/1.5/2.0/2.5/3.0							

mean values were used.

Crystal structures of the fibers were determined using an X-ray diffraction analyzer (X'Pert PRO MPD, PANalytical, Netherlands) operated at 40 kV and 40 mA with Ni-filtered Cu Kα radiation. The data were collected over the 2θ range from 10-90 ^{o} at a scan rate of 4 ^{o} min^{-1} in the equatorial and meridian scan, and the data of the azimuth scan (002) were collected over the range from 90-270 ^{o} at a scan rate of 6 ^{o} min^{-1}. The apparent crystallite size was calculated from the baseline corrected and resolved peak profiles. Each sample was measured five times, and the mean values were used. The XRD diffraction patterns were curve-fitted to a Lorentz-Gauss area function using the software of Peak Fit v4.12 to acquire the parameters of peak position, peak intensity, and full width at half maximum height (FWHM). The diffraction peak positions and the full widths at half maximum (FWHM) were used to calculate the crystallite size by the Scherrer equation:

$$L(nlk) = K\lambda/B\cos\theta \quad (1)$$

where θ is the diffraction peak position of the (*nlk*) plane; λ=0.15406 nm is the wavelength of the X-rays; *B* is the FWHM of the peak (rads); and *K* is the Scherrer geometric factor, or shape factor. The crystallite correlation lengths along the fiber axis ($La_{\parallel}$) and perpendicular to the fiber axis ($La_{\perp}$) were determined by the (100) diffraction peak of the meridian scan and the equatorial scan, respectively. The shape factor *K* is 1.84 for La. The thickness of the carbon crystallite (Lc) was determined by the (002) diffraction peak of the equatorial scan, and the shape factor *K* is 0.89 for Lc.

The orientation angle was calculated from the azimuth scan data. According to the calculation method of Herman's orientation factor, the following two equations were obtained:

$$\langle\cos^2\Phi_{a,z}\rangle = \frac{\int_0^{\pi/2} I(\Phi)\cos^2\Phi\sin\Phi d\Phi}{\int_0^{\pi/2} I(\Phi)\sin\Phi d\Phi} \quad (2)$$

$$\cos^2\Phi_{a,z} + \cos^2\Phi_{b,z} + \cos^2\Phi_{c,z} = 1 \quad (3)$$

where $I(\Phi)$ is the azimuthal intensity distribution function of the (100) diffraction; and $\Phi_{a,z}$, $\Phi_{b,z}$ and $\Phi_{c,z}$ are the angles between one of the normal vectors of the lattice plane (i.e., vectors **a**, **b** and **c**) and the fiber axial direction (i.e., **z**), respectively [13,14]. Because the structure along the fiber radial direction should be isotropic, there should be the relation

$$\langle\cos^2\Phi_{a,z}\rangle = \langle\cos^2\Phi_{b,z}\rangle \quad (4)$$

By combining equation (2), (3), and (4), $\langle\cos\Phi^2_{c,z}\rangle$ could be obtained, where $\Phi_{c,z}$ is the orientation angle between the graphite layers and the fiber axis.

The dispersion of the carbon structure in the carbon fibers was observed using a high-resolution transmission electron microscope (HRTEM; ARM-1250, JEOL, Japan) with an acceleration voltage of 300 kV. For this observation, the fiber was cut into powder and placed in an agate mortar to grind. The ground powder was then mixed with anhydrous ethanol in a 1:99 weight ratio to form a solution. After ultrasonic treatment, the solution was dropped onto a micro-grid and left to evaporate the solvent for about 5 min before testing.

Results and Discussion

Effect of PAN-CF Physical Structure Changes on Its High-temperature Stretching Deformation Ability

In a high-temperature environment, and especially when the temperature is higher than 2000 ^{o}C, the PAN-CF can be deformed by stretching, where it undergoes complex physical and chemical changes during the high-temperature treatment. To clarify the effect of the physical structure changes of the PAN-CF on its high-temperature stretching deformation while simultaneously avoiding the influence of chemical changes, the stretching deformation of PAN-CF was studied at a temperature lower than the preparation temperature. Because the stretching deformation capacity of PAN-CF was great at 2000 ^{o}C and above, the testing temperature was designed to be not less than 2000 ^{o}C, while limiting the preparation temperature of the PAN-CF sample to be above 2000 ^{o}C.

Effect of Temperature and Tension on the Stretching Deformation Ability of PAN-CF with Physical Structure Changes

Only the physical structure was changed when the PAN-CF was heat-treated in temperatures below the preparation temperatures. The stretching tension of the P-24 fiber increased with increasing relative draft ratio when stretched

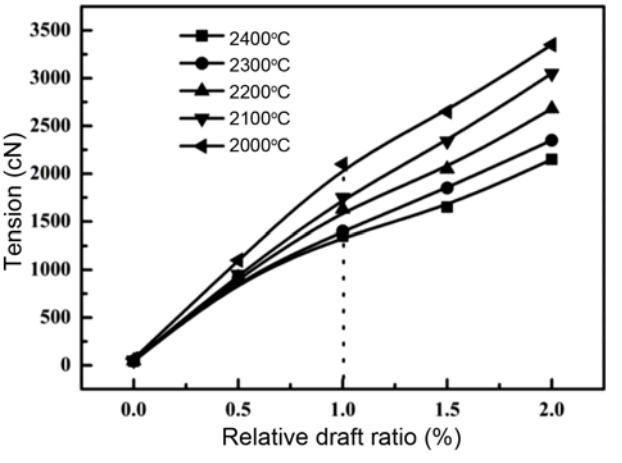

Figure 2. Tension of P-24 fiber as a function of relative draft ratio for various testing temperatures.

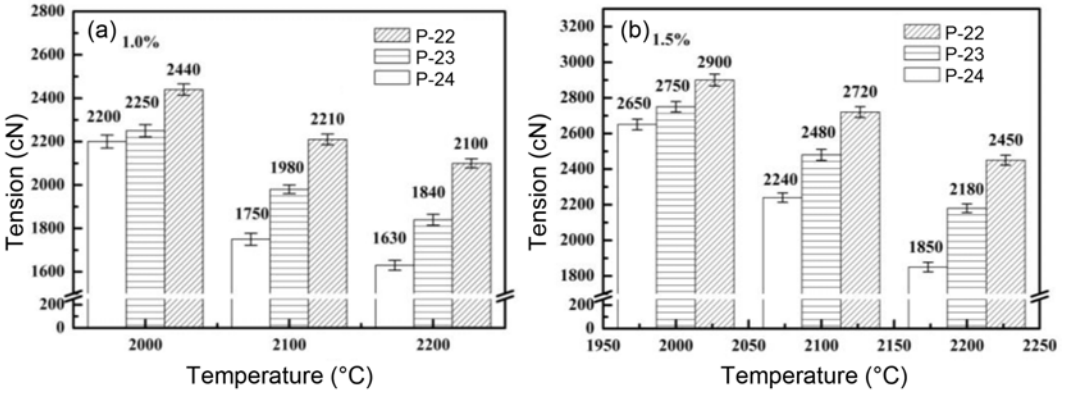

Figure 3. Fiber tension for three samples with varying preparation temperatures under a relative draft ratio of (a) 1.0 % and (b) 1.5 %.

in temperatures range of 2000-2400 °C, as shown in Figure 2. When the relative draft ratio was greater than 1.0 %, however, the tendency of the stretching tension increase reduced as a function of relative draft ratio Figure 2. As the testing temperature increased, the stretching tension of the PAN-CF decreased. Specifically, when the relative draft ratio was 1.0 %, the corresponding tensions were 2200 and 1400 cN at testing temperatures of 2000 and 2400 °C, respectively, exhibiting an obvious effect of the temperature on the stretching deformation of PAN-CF. At the same time, as the relative draft ratio increased, the difference of the stretching tension value of PAN-CF for various testing temperatures was greater, which also indicates that the effect of temperature on the stretching deformation of PAN-CF is enhanced under a large relative draft ratio.

The degree of structural regulation of the PAN-CF is greater with a higher preparation temperature. Stretching tension tests were carried out on the P-24, P-23 and P-22 fibers with preparation temperatures of 2400, 2300 and 2200 °C, respectively, and relative draft ratios of 1.0 % (Figure 3(a)) and 1.5 % (Figure 3(b)). The effect the structural regularity of PAN-CF has on its stretching deformation was further studied. Under the same testing conditions, the stretching tension of the P-24 fiber was low, which indicated that the stretching deformation ability of PAN-CF with a relatively higher regulation structure was greater, as shown in Figure 3.

Comparing the stretching tensions for the three different PAN-CF samples at the same testing temperature in Figures 3(a) and 3(b), it can be seen that a larger relative draft ratio induces a greater dependence of the tension on the carbon structural regularity. The stretching tension of the P-23 and P-24 fibers with a relative draft ratio of 1.0 % (Figure 3(a)) were 1840 and 1630 cN, respectively, for a difference of 210 cN; while for a relative draft ratio of 1.5 % (Figure 3(b)) the difference was 330 cN. The above studies indicate that, with an increase in the relative draft ratio, the PAN-CF possessing a more regular carbon structure can better reflect the effect of temperature and tension on the stretching deformation.

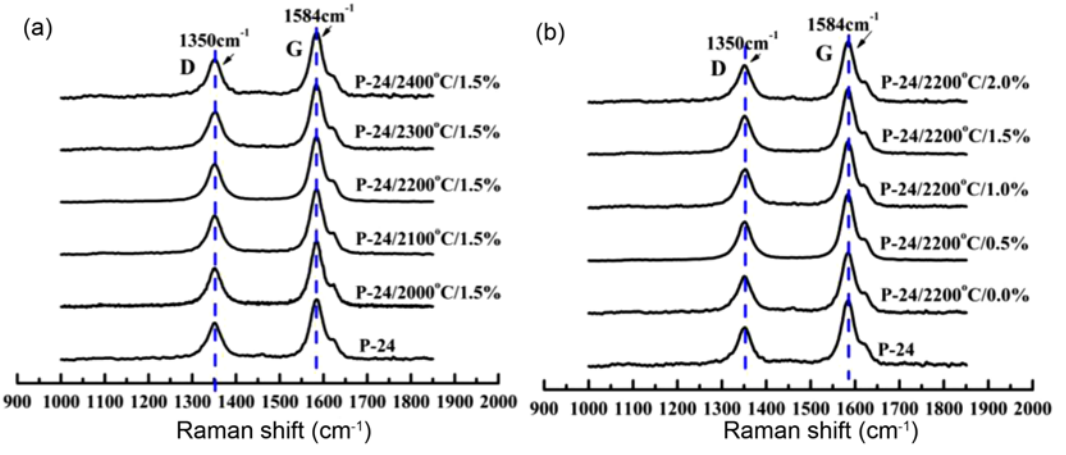

Figure 4. The Raman spectra of P-24 fiber as well as P-24 fiber after different retreated conditions; (a) 2000-2400 °C 1.5 % and (b) 2200 °C 0.0-2.0 %.

Correlation between Physical Structure Changes of PAN-CF and Its Stretching Deformation Capability

The same PAN-CF samples exhibited different stretching deformation abilities under different testing conditions, while different PAN-CF sample types also exhibited different stretching deformation ability under the same testing conditions. These differences in stretching deformation abilities were related to the carbon structure of the PAN-CF.

In theory, if the treatment time was appropriate, there would not be chemical reaction in the carbon fibers when the retreated temperature was not higher than the preparation temperature. Taking the P-24 fiber as an example, the changes of the chemical structure in the fibers were analyzed, when the fibers were retreated under the different conditions.

The Raman spectra of P-24 fiber after stretching in temperatures range of 2000-2400 °C at a relative draft ratio of 1.5 % are shown in Figure 4(a). The Raman spectra of P-24 fiber after stretching in a relative draft ratio range of 0-2.0 % at 2200 °C are shown in Figure 4(b). As shown in Figure 4, there were two characteristic peaks in Raman spectra band, and they were the D peak around 1350 cm^{-1} and the G peak around 1584 cm^{-1}. After retreated under different conditions, the two Raman band peak positions of the fibers were basically unchanged.

The data of peak position and FWHM in the Figure 4 as well as the Ra values which are the ratio of the D peak area to that of the G peak are also shown in the Table 4, and they were nearly unchanged. Therefore, when the fibers were retreated under a temperature which was not higher than their preparation temperatures, the stretching ability of the fibers would not be related to the chemical structure changes, but related to their own structures as well as the physical structure changes.

The carbon crystallites in the PAN-CF can be regarded as macromolecules that, when heated, are more active than in equilibrium. When a carbon crystallite absorbs enough energy it can overcome its translational or rotational energy barrier and, if a tension force is simultaneously applied, the carbon crystallite can be oriented in the direction of the external force.

Unlike other microcrystalline structures, the microcrystals in carbon fibers participate in thermal motion with their own structural characteristics, as shown in Figure 5. First, the carbon crystallites in the carbon fiber are not isolated, exhibiting many amorphous cross-linking structures between the carbon crystallites. In the Raman spectra, the G-peak signal represents a regularly-ordered carbon-sp^2 hybrid structure, and the D-peak signal represents a defect, boundary, or carbon-sp^3 hybrid structure. The G-peak signal can reflect the microcrystalline structure, while the D-peak signal can

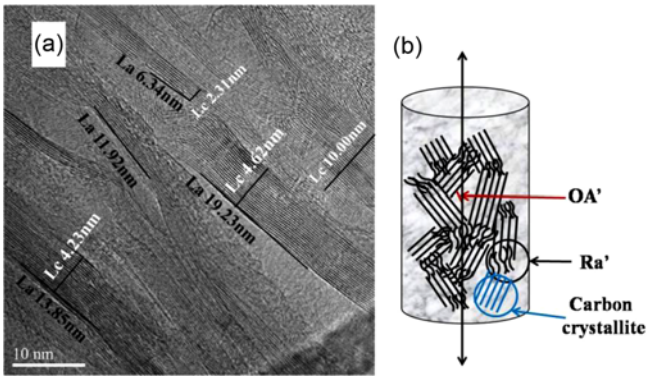

Figure 5. (a) HRTEM image observation of carbon crystallite grain size dispersion in P-24 fiber and (b) schematic diagram of carbon microcrystalline characteristics in PAN-CF.

Table 4. The raman band peak parameters of P-24 fiber before and after retreated under different conditions

Relative draft ratio (%)	Retreated temperature (°C)	D shift (cm^{-1})	FWHM(D) (cm^{-1})	G shift (cm^{-1})	FWHM(G) (cm^{-1})	Ra
-	-	$1350.42^{+0.19}_{-0.18}$	$40.27^{+0.43}_{-0.54}$	$1583.97^{+0.10}_{-0.09}$	$38.39^{+0.33}_{-0.28}$	$0.57^{+0.006}_{-0.002}$
	2000	$1350.42^{+0.11}_{-0.14}$	$40.05^{+0.38}_{-0.48}$	$1584.00^{+0.08}_{-0.11}$	$38.08^{+0.29}_{-0.34}$	$0.57^{+0.003}_{-0.004}$
	2100	$1349.78^{+0.23}_{-0.17}$	$39.61^{+0.55}_{-0.44}$	$1583.91^{+0.12}_{-0.07}$	$38.28^{+0.31}_{-0.36}$	$0.57^{+0.002}_{-0.004}$
1.5	2200	$1350.34^{+0.04}_{-0.08}$	$39.87^{+0.49}_{-0.41}$	$1584.55^{+0.09}_{-0.07}$	$37.85^{+0.34}_{-0.33}$	$0.57^{+0.003}_{-0.005}$
	2300	$1349.58^{+0.10}_{-0.05}$	$40.13^{+0.37}_{-0.47}$	$1584.21^{+0.10}_{-0.11}$	$37.98^{+0.35}_{-0.29}$	$0.57^{+0.004}_{-0.006}$
	2400	$1349.68^{+0.07}_{-0.02}$	$39.74^{+0.58}_{-0.45}$	$1584.23^{+0.07}_{-0.09}$	$38.12^{+0.28}_{-0.27}$	$0.57^{+0.002}_{-0.004}$
0.0		$1350.14^{+0.20}_{-0.24}$	$40.07^{+0.46}_{-0.39}$	$1584.22^{+0.06}_{-0.07}$	$38.09^{+0.30}_{-0.26}$	$0.57^{+0.003}_{-0.001}$
0.5		$1350.02^{+0.18}_{-0.21}$	$40.14^{+0.33}_{-0.43}$	$1584.13^{+0.09}_{-0.11}$	$38.02^{+0.31}_{-0.25}$	$0.57^{+0.003}_{-0.004}$
1.0	2200	$1350.28^{+0.13}_{-0.17}$	$39.91^{+0.51}_{-0.42}$	$1584.31^{+0.003}_{-0.004}$	$37.96^{+0.29}_{-0.28}$	$0.57^{+0.002}_{-0.005}$
1.5		$1350.34^{+0.04}_{-0.08}$	$39.87^{+0.49}_{-0.41}$	$1584.55^{+0.09}_{-0.07}$	$37.85^{+0.34}_{-0.33}$	$0.57^{+0.003}_{-0.005}$
2.0		$1350.27^{+0.12}_{-0.15}$	$39.92^{+0.52}_{-0.41}$	$1584.36^{+0.12}_{-0.07}$	$37.99^{+0.31}_{-0.30}$	$0.57^{+0.003}_{-0.002}$

reflect the intermittent cross-linked structure between microcrystals. The graphitization degree Ra is the ratio of the D peak area to that of the G peak, where a larger Ra value indicates a more disorderly cross-linking structure existing between the carbon crystallites in the PAN-CF. Second, the orientation degree of carbon crystallites is not very good in the fiber, there are orientation angles between the crystallites and the fiber axis. Third, the carbon structure in PAN-CF is discrete where almost every microcrystal has its own independent characteristics, including grain size, orientation angle (OA') and cross-linking structure (Ra').

For different carbon microcrystals in the same carbon fiber, a smaller degree of cross-linking Ra' between carbon crystallites indicates a lower carbon crystallite movement energy barrier. Further, a smaller orientation angle OA' of the carbon crystallite indicates a reduced movement resistance of the carbon crystallites. Finally, a smaller carbon crystallite grain size indicates a greater movement ability of the carbon crystallites. Thus, when the Ra', OA' and grain size are small, the movement energy barrier of the carbon crystallites is low. For the same carbon fiber, when the PAN-CF testing temperature is low or the stretching tension is small, only the microcrystals with lower kinetic energy barrier participate in the movement (as shown in region (1) of Figure 6) and the high-temperature stretching deformation ability of the PAN-CF is poor. As the testing temperature or the relative draft ratio is increased, however, more carbon crystallites with higher kinetic energy barrier (i.e., region (2) in Figure 6) are able to take part in the movement, thus enhancing the high-temperature stretching deformation ability of PAN-CF, as shown in Figure 2 for the P-24 fiber.

For different PAN-CF samples, the relationship between the PAN-CF stretching tension and its structure was studied by analyzing the structures of the P-24, P-23 and P-22 fibers when the relative draft ratio was 1.5 % and the testing temperature was 2200 °C. The basic structural parameters of the P-24, P-23 and P-22 fibers are shown in Table 5.

It can be seen from Table 5 that, as the PAN-CF preparation temperature increases, the degree of cross-linking, orientation angle and carbon crystallite volume changes. The carbon crystallite volume was calculated by multiplying $La_{\parallel}$, $La_{\perp}$ and Lc. The degree of cross-linking, orientation angle and stretching tension gradually became smaller, but the carbon crystallite volume became larger. According to this analysis, the movement resistance of the carbon crystallites in the PAN-CF sample exhibiting a lower degree of cross-linking, smaller orientation angle and smaller carbon crystallite volume was smaller, and the stretching deformation ability of the PAN-CF was greater. The stretching tension of the P-24 fiber in Table 5 remained small under the influence of its relatively large carbon crystallite volume, which indicated that the main structural parameters affecting the relative movement of carbon crystallites in PAN-CF were the degree of cross-linking (Ra) between carbon crystallites and the orientation angle (OA) of the carbon crystallites.

At the same time, when the preparation temperature was high, the carbon crystallites in PAN-CF were large enough to

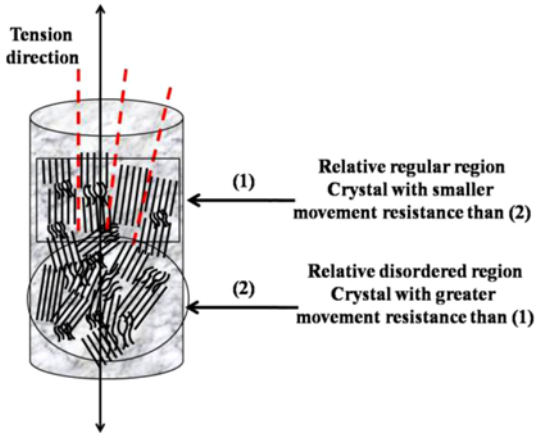

Figure 6. Schematic diagram of the carbon crystallites possessing different movement ability.

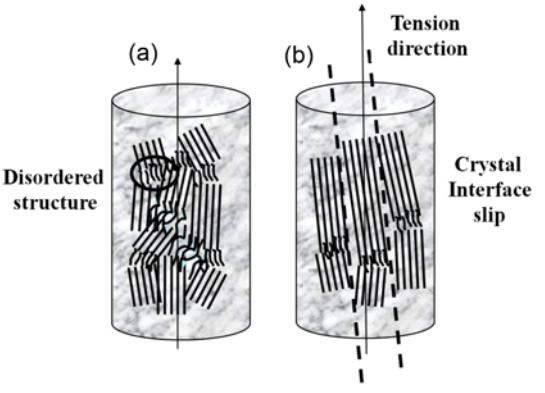

Figure 7. Comparision schematic diagram of stretching slippage movement capability of carbon microcrystalline.

Table 5. Basic structural parameters of PAN-CFs and the stretching tensions (testing conditions: 2200 °C, 1.5 % relative draft ratio)

Sample no.	Ra	OA (°)	$La_{\parallel}$ (nm)	$La_{\perp}$ (nm)	Lc (nm)	Carbon crystallite volume (nm^3)	Tension (cN)
P-24	$0.57^{+0.003}_{-0.004}$	$16.51^{+0.03}_{-0.05}$	$13.593^{+0.043}_{-0.055}$	$7.766^{+0.036}_{-0.064}$	$4.144^{+0.043}_{-0.024}$	437.45	1850^{+23}_{-25}
P-23	$0.72^{+0.003}_{-0.002}$	$16.71^{+0.05}_{-0.04}$	$12.386^{+0.064}_{-0.066}$	$7.187^{+0.058}_{-0.035}$	$3.733^{+0.036}_{-0.018}$	332.30	2180^{+30}_{-10}
P-22	$0.83^{+0.004}_{-0.005}$	$17.14^{+0.06}_{-0.02}$	$11.326^{+0.075}_{-0.078}$	$6.892^{+0.046}_{-0.024}$	$3.450^{+0.026}_{-0.041}$	269.30	2450^{+25}_{-35}

effectively transfix the fiber, and the grain boundary structure was more clear and coherent while the cross-linking between the carbon crystallites was weakened. The carbon crystallites were prone to relative slip motion when an external force was applied. In Figure 7, for example, the preparation temperature of sample B was higher than that of sample A, and the carbon crystallites in sample B slipped easily when the sample was stretched. Therefore, the high-temperature stretching deformation performance of sample B was better than that of sample A.

Effect of Physical and Chemical Structure Changes on the High-temperature Stretching Deformation Ability of PAN-CF

In the PAN-CF preparation process, increasing the orientation degree of the target PAN-CF was typically achieved by stretching the PAN-CF at a temperature higher than the preparation temperature. In this study, the stretching deformation was different from the previous one in that, with a testing temperature greater than the preparation temperature, the PAN-CF underwent both physical and chemical changes.

With increasing PAN-CF preparation temperature, the non-carbon element content in the PAN-CF gradually decreased, as shown in Table 1. When the preparation temperature rose to ≥1900 °C, there were almost no non-carbon elements detected in the PAN-CF. According to the evolution of the PAN-CF prepared at different temperatures, two categories were detected: nitrogen-free PAN-CF and nitrogen-containing PAN-CF, where the high-temperature evolution of the two categories of PAN-CF was different. To avoid the influence of nitrogen removal on the stretching deformation of PAN-CF, the effect of the physical and chemical structural changes on the stretching deformation of PAN-CF was carried out using a segmented study.

Effect of Physical and Chemical Changes on the High-temperature Stretching Deformation Ability of Nitrogen-free PAN-CF

The PAN-CFs with different initial structures were further stretched at 2400 °C, whose structural parameters are shown in Table 6 and stretching tension curve is shown in Figure 8. The P-24 fiber experienced physical structure changes at 2400 °C and its stretching tension continued to be high, so its stretching deformation ability was poor. The other nitrogen-free PAN-CF samples (as shown in Figure 8) experienced both physical and chemical structure changes and their stretching tension were low, so their stretching deformation abilities were great. If the chemical change was not considered then the results of Figure 8 would be contrary to the results of Figure 3, which indicated that the chemical structure changes of the PAN-CF was essential for the stretching deformation ability enhancement.

The P-24 fiber had the characteristics of smaller Ra, smaller OA and larger grain size than the other PAN-CF samples. Further, the cross-linking weak bonds in the P-24 PAN-CF did not break when tested at 2400 °C. Although the OA of the carbon crystallites in P-24 fiber was small, the two negative factors of its large grain size and connected cross-linking between carbon crystallites resulted in its poor stretching deformation ability. In the other PAN-CF samples exhibiting chemical structure changes, a lower preparation temperature signified a lower stretching tension. The structural characteristics of the PAN-CF samples with lower preparation temperatures were a smaller crystallite size and more cross-linking, as shown in Table 6.

When the temperature was higher than the preparation temperature, the breaking of weak bonds (as shown in Figure 9) in the more numerous cross-linking structures of

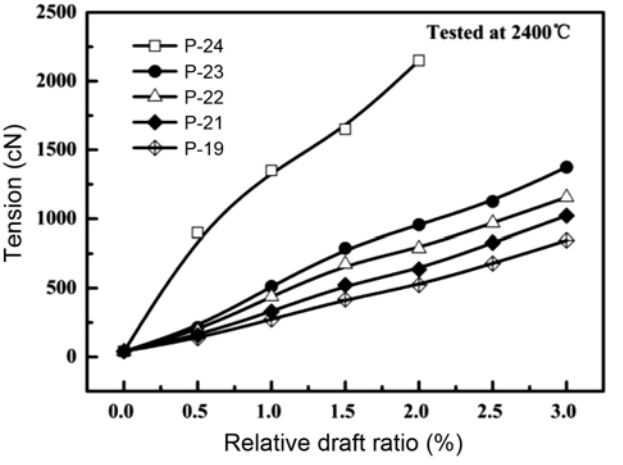

Figure 8. The tension as a function of the relative draft ratio of nitrogen-free PAN-CF of various structures tested at 2400 °C.

Table 6. Basic structural parameters of PAN-CF with different preparation temperatures

Sample no.	Ra	$La_{\parallel}$ (nm)	$La_{\perp}$ (nm)	Lc (nm)	OA (°)
P-24	$0.57^{+0.003}_{-0.004}$	$13.593^{+0.069}_{-0.055}$	$7.766^{+0.036}_{-0.064}$	$4.144^{+0.043}_{-0.024}$	$16.51^{+0.03}_{-0.05}$
P-23	$0.72^{+0.003}_{-0.002}$	$12.386^{+0.064}_{-0.066}$	$7.187^{+0.058}_{-0.035}$	$3.733^{+0.036}_{-0.018}$	$16.71^{+0.05}_{-0.04}$
P-22	$0.83^{+0.004}_{-0.005}$	$11.326^{+0.075}_{-0.078}$	$6.892^{+0.046}_{-0.024}$	$3.450^{+0.026}_{-0.041}$	$17.14^{+0.06}_{-0.02}$
P-21	$0.98^{+0.006}_{-0.002}$	$10.353^{+0.038}_{-0.068}$	$6.880^{+0.039}_{-0.028}$	$3.192^{+0.025}_{-0.017}$	$17.51^{+0.07}_{-0.06}$
P-19	$1.17^{+0.005}_{-0.007}$	$8.151^{+0.052}_{-0.048}$	$5.981^{+0.035}_{-0.040}$	$2.450^{+0.020}_{-0.033}$	$19.74^{+0.05}_{-0.04}$

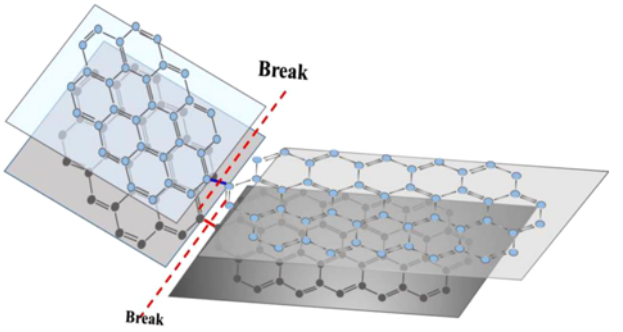

Figure 9. Schematic diagram of the high-temperature weak-bonded breaking of carbon crystallites.

PAN-CF caused the small carbon crystallites to absorb energy and move rapidly under stretching, thus realizing the PAN-CF stretching deformation. Further, the effect of fiber shrinkage on the stretching deformation of the PAN-CF during the carbon crystallite growth process was weak and could be neglected. Therefore, when the temperature was higher than the preparation temperature, under the influence of physical and chemical structure changes, a larger Ra value of nitrogen-free PAN-CF indicated a better stretching deformation ability.

Effect of Physical and Chemical Changes on the High-temperature Stretching Deformation Ability of Nitrogen-containing PAN-CF

According to the contents of nitrogen and hydrogen elements in Table 1, the hydrogen content was relatively little, which could be neglected. To further clarify the effect of the chemical structure change caused by the removal of non-carbon atoms on the stretching deformation of PAN-CF, the relationship of stretching tension and relative draft ratio of PAN-CF with different nitrogen contents tested at 2400 °C is shown in Figure 10. The nitrogen content of the PAN-CF

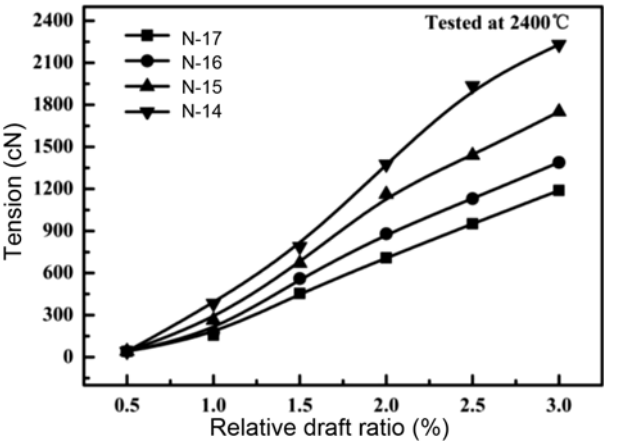

Figure 10. Tension as a function of relative draft ratio of PAN-CF samples containing different nitrogen contents tested at 2400 °C.

with different preparation temperatures is shown in Table 1.

When stretched at the same relative draft ratio, the stretching deformation of the N-17 fiber with a lower Ra and larger grain size, as shown in Table 7, was better in Figure 10 than the other fibers. This seemed contradictory to the results of Figure 8, which was related to the nitrogen element in PAN-CF. However, with increasing preparation temperature the nitrogen content in the PAN-CF decreased, as shown in Table 1. The nitrogen content of the N-17 fiber was the lowest in the nitrogen-containing samples.

When the nitrogen-containing PAN-CF was tested at 2400 °C, two forces existed that affect its stretching deformation. On the one hand, the breakage of a large amount of cross-linking weak bonds enhances the carbon crystalline movement ability. On the other hand, many nitrogen atoms in the PAN-CF will be quickly removed under the high temperature used. After the removal of nitrogen, a large number of dangling bonds existed in the carbon hexagonal

Table 7. Basic structural parameters of PAN-CFs with different nitrogen contents

Sample no.	Ra	$La_{\parallel}$ (nm)	$La_{\perp}$ (nm)	Lc (nm)	OA (°)
N-17	$1.208^{+0.002}_{-0.003}$	$6.394^{+0.039}_{-0.020}$	$5.783^{+0.027}_{-0.012}$	$2.022^{+0.023}_{-0.010}$	$20.10^{+0.03}_{-0.06}$
N-16	$1.210^{+0.004}_{-0.001}$	$6.394^{+0.026}_{-0.031}$	$5.783^{+0.014}_{-0.023}$	$2.022^{+0.012}_{-0.030}$	$20.53^{+0.02}_{-0.05}$
N-15	$1.232^{+0.003}_{-0.005}$	$5.672^{+0.033}_{-0.062}$	$5.260^{+0.032}_{-0.024}$	$1.937^{+0.032}_{-0.029}$	$20.92^{+0.09}_{-0.04}$
N-14	$1.242^{+0.005}_{-0.002}$	$5.130^{+0.042}_{-0.039}$	$5.129^{+0.037}_{-0.028}$	$1.798^{+0.021}_{-0.030}$	$21.44^{+0.05}_{-0.06}$

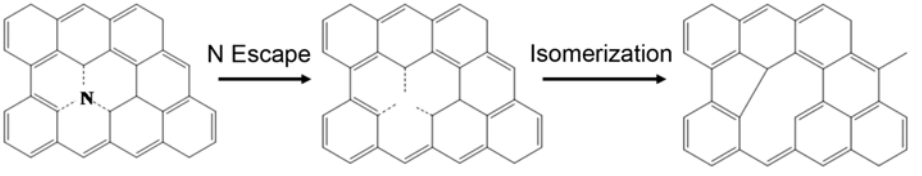

Figure 11. Schematic diagram of nitrogen atom elimination process at high temperature.

ring and, because these dangling bonds were very unstable, the atoms quickly rearranged to reduce the overall energy. At the same time, the carbon structure quickly underwent isomerization reaction, which caused carbon hexagonal ring shrinkage in the graphite layer and interlayer, and thus resulted in an increased movement resistance of the carbon crystallites. A schematic diagram of the process of nitrogen atom elimination at high temperature is shown in Figure 11. The combined effects of the above phenomena influenced the stretching deformation ability of PAN-CF, and therefore the stretching deformation ability of the PAN-CF with a lower nitrogen element content was great.

Conclusion

The PAN-CF high-temperature stretching deformation was found to be fundamentally the result of the relative slip movement of carbon crystallites. The stretching deformation ability of different PAN-CF samples was related to the cross-linking degree of the carbon crystallites, the OA of the carbon crystallites and the nitrogen content, and was also related to the physical and chemical changes taking place in the structure. When the PAN-CF experienced physical structure changes, a reduced degree of cross-linking between the crystallites or reduced OA signified easier slipping of the crystallites. In the same environment, a reduced stretching tension signified an improved stretching deformation ability. Therefore, a higher preparation temperature of nitrogen-free (<0.15 wt%) PAN-CF signified an improved stretching deformation ability, when tested under the temperature lower than the preparation temperature. When the PAN-CF experienced physical and chemical structure changes, the microcrystalline cross-linking in the PAN-CF was prone to fracture and slipping, and so the high-temperature stretching deformation ability was enhanced. These samples contained more cross-linking structures, which were more unstable in the nitrogen-free PAN-CF of lower preparation temperature, and thus more fracturing of weak bonds, causing a reduced stretching tension. For nitrogen-containing PAN-CF, the removal of nitrogen led to severe shrinkage in the graphite layer and interlayer and an increase in the fiber tension, and thus the high-temperature stretching deformation ability of the PAN-CF samples with reduced nitrogen content was improved.

Acknowledgments

Financial support from the National High Technology Research and Development Program of China (“863 Program” Grant No.:2015AA03A202) and “Fundamental Research Funds for the Central Universities ZY 1609”) is gratefully acknowledged.

References

1. H. J. Wang, H. F. Wang, D. F. Li, X. M. Zhu, F. He, and X. K. Wang, *New Carbon Mater.,* **20**, 157 (2005).
2. A. J. Gao, C. Zhao, S. Luo, Y. J. Tong, and L. H. Xu, *Mater. Lett.,* **65**, 3444 (2011).
3. W. P. Chang, Z. M. Shen, and Q. Wang, *New Carbon Mater.,* **13**, 28 (1998).
4. D. F. Li, H. J. Wang, L. B. Xue, and X. K. Wang, *Chem. Ind. Eng. Prog*., **25**, 1101 (2006).
5. Z. Y. Xu, H. B. Liu, Y. C. Su, R. Z. Yang, and W. Z. Gong, *Carbon*, **3**, 4 (1997).
6. H. B. Liu, H. B. Zhang, Y. W. Zheng, and Z. Y. Xu, *J. HuNan Univ.,* **22**, 55 (1995).
7. X. Y. Qin, Y. G. Lu, W. Z. Zhao, and H. Xiao, *J. Mater. Sci.,* **49**, 5017 (2014).
8. L. B. Xue, H. J. Wang, and D. F. Li, *New Carbon Mater.,* **21**, 243 (2006).
9. H. B. Zhang, Ph. D. Dissertation, HNU, Changsha, 1998.
10. Z. Y. Xu, H. B. Liu, H. B. Zhang, Y. C. Su, and R. G. Xiong, *Carbon*, **1**, 1 (1995).
11. Z. Q. Liu, *New Carbon Mater.,* **2**, 7 (1992).
12. H. B. Zhang, H. B. Liu, and Z. Y. Xu, *Hi-Tech Fiber Appl.,* **26**, 6 (2001).
13. L. Li, M. F. Wang, N. Jiao, L. H. Xu, and W. Y. Cao, *Chin. Polym. Bull.,* **1**, 43 (2014).
14. Y. R. Zhou, X. Han, X. Y. Hu, L. H. Xu, and W. Y. Cao, *High Perform. Polym.,* **29**, 1158 (2017).